Independently Commanding Size, Shape and Orientation of Robot Endpoint Stiffness in Tele-Impedance by Virtual Ellipsoid Interface

Peternel, Luka; Beckers, Niek; Abbink, David A.

DOI
10.1109/ICAR53236.2021.9659430

Publication date
2021

Document Version
Accepted author manuscript

Published in
Proceedings of the 2021 20th International Conference on Advanced Robotics (ICAR)

Independently Commanding Size, Shape and Orientation of Robot Endpoint Stiffness in Tele-Impedance by Virtual Ellipsoid Interface

Luka Peternel*, Niek Beckers, and David A. Abbink

***Abstract*— The existing state-of-the-art interfaces for commanding a remote robot's endpoint stiffness ellipsoid in tele-impedance lack the ability to independently control its size, shape and orientation or they are not easily to implement due to the use of physiological signals, such as electromyography, to control the endpoint stiffness. We propose a novel method that can command size, shape and orientation independently and simultaneously through a virtual stiffness ellipsoid generated on a touchscreen device. The human operator controls size, shape and orientation of the virtual ellipsoid using his/her index and thumb fingers of one hand. This virtual ellipsoid is then mapped to the Cartesian stiffness ellipsoid of a remote robot endpoint in real-time. The other hand holds the haptic device to control the pose of the remote robotic arm. Compared to the state-of-the-art methods to control the robot stiffness in tele-impedance, the main advantages of the proposed method are its relatively simple implementation and ability of independent control over various aspects of the robot endpoint stiffness ellipsoid. To provide a proof-of-concept and demonstrate the main features of the proposed approach, we performed several experiments on a tele-impedance setup with a Kuka LBR iiwa robotic arm and a Force Dimension Sigma7 haptic device. We examined two principal types of tasks, in which changing stiffness parameters of the remote robot is important for successful task execution: counteracting external perturbations and establishing contact with unknown objects. The results indicate that our proposed approach can successfully deal with these tasks. A human subject study showed that the touchscreen interface is faster in commanding the desired stiffness compared to another state-of-the-art input method, while showing similar workload ratings.**

I. Introduction

We often strive to make robots autonomous so they can produce various tasks independently from humans. However, in some cases the human involvement and supervision is preferred or even necessary. Prominent examples include robot-assisted surgery, space robotics and rescue robotics. In such cases, teleoperation is the key method to enable human involvement into the control over the robot's actions.

In a classical teleoperation setup, the human operator can control the movement of a remote humanoid robot's arm (slave) with the movement of his/her own arm through an interface (master). The measured pose on the master is used to command the reference pose of the slave. A high gain position controller on the remote humanoid robot ensures accurate tracking of the commanded reference pose. However, due to the stiff properties of the robotic arm under such a control method, operating in a remote environment that is unknown or unpredictable, such as disaster areas or different homes, could result in high interaction forces and unsafe situations.

The authors are from the Delft Haptics Lab, Cognitive Robotics, Delft University of Technology, Mekelweg 2, 2628 CD Delft, The Netherlands.
*Corresponding author (e-mail: l.peternel@tudelft.nl)

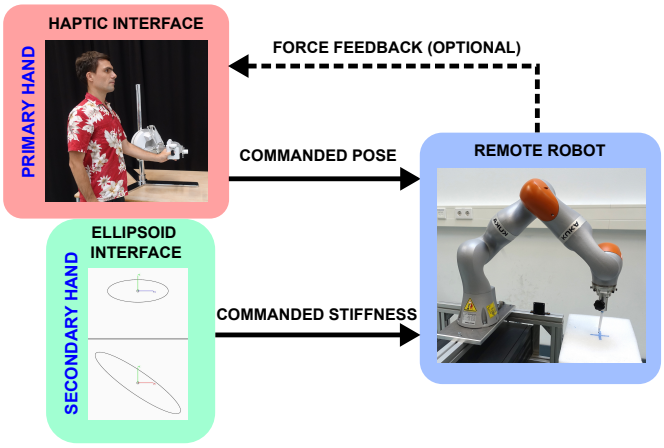

Fig. 1: Tele-impedance block scheme with the proposed stiffness-command interface. The human operator controls the pose of the remote robot (Kuka LBR iiwa) with the movements of his/her primary hand controlling a haptic device (Force Dimension Sigma7). The impedance of the remote robot is controlled by the secondary hand through the proposed virtual ellipsoid interface that shows the size, shape and orientation of the robot's Cartesian stiffness ellipsoid. Although not implemented in the current study, the measured force at the remote robot could then be used as a force-feedback, which is reproduced at the human operator's arm by the haptic device.

Humans have the ability to adjust the impedance of their arm endpoint in order to improve the task execution in unknown and unpredictable environments [1], [2]. In addition, adjusting the endpoint impedance is also important in executing various collaborative tasks [3], [4]. To enable the human operator to control the endpoint stiffness of the remote robot arm in teleoperation, the concept of tele-impedance was developed [5]–[7]. This concept extends classical teleoperation with an additional command channel that enables real-time adjustments of the remote robot's impedance. Endpoint impedance can be changed with [6], [8]–[10] or without [5], [7], [11] feedback to the human operator about the forces experienced by the remote robot.

In methods employing machine learning and robot autonomy to set the remote robot's endpoint stiffness, such as [12]–[14], the human has limited control over the robot's impedance. As argued in [8], the main advantage of giving the human operator direct control over the remote robot impedance is that the human can use his/her cognitive capabilities and experience to adopt a suitable impedance strategy tailored to specific and possibly dynamic tasks requirements or conditions.

The crucial element of tele-impedance is the interface at the master side that enables the human to control the

impedance of the slave robot endpoint. One approach employs electromyography (EMG) to measure the muscle activity in the human operator's pose and the arm pose in order to estimate the size, shape and orientation of the stiffness ellipsoid at the endpoint and command it to the operated robot [5]. Another approach estimates muscle activity by measuring changes in muscle morphology through electrical impedance tomography (EIT) [15]. However, while the size, shape and orientation can be estimated, the human operator cannot always change them independently because of their dependency on the arm configuration [16], [17] and a strong coupling between muscle activities through synergies [18]–[20]. Therefore, the ability to command the size, shape and orientation of the stiffness ellipsoid to the robot is limited. In addition, it has been shown that there is a coupling effect between the interaction force at the haptic interface and human commanded stiffness in EMG-based tele-impedance [21]. Furthermore, these approaches typically involve a complex setup (including issues related to wearable devices [22], [23]) and a time-consuming calibration process, which is another key disadvantage in terms of applicability.

In order to address the applicability concerns, several more practical impedance-command interfaces were developed. In [6], [11], the authors proposed to use an interface based on measuring the hand grip force. When the human operator squeezes their hand, the remote robot becomes stiffer. However, a force sensor is still relatively expensive equipment and maintaining a constant grip force may lead to unnecessary physical fatigue. To avoid this issue, a novel hand-held interface was proposed in [8] that enables the human operator to control the remote robot impedance with a finger on a linear push button. While these existing non-EMG based interfaces are much more practical and easily applicable, they typically have only one degree of freedom (DoF). As a result, they can only scale the size of the stiffness ellipsoid, but cannot change its shape and orientation (that is, without any additional complex arm-configuration measurements [16]).

To enable *independent* and simultaneous commanding of *all aspects* of the stiffness ellipsoids at the remote robot and at the same time maintain low-cost and applicability, we propose a novel multi-DoF method to control a remote robot's endpoint stiffness in tele-impedance based on a virtual stiffness ellipsoid concept. The human operator forms and manipulates the virtual ellipsoid with the fingers of secondary arm to adjust the size, shape and orientation of the remote robot's endpoint stiffness ellipsoid. In this study we use a commercially available touchscreen device as an interface to generate the virtual stiffness ellipsoid. Simultaneously the operator holds a haptic device with the primary arm to control the reference pose of the remote robot's endpoint. The pose and impedance commands are then sent to the remote robot in real-time. While the proposed interface may not be as intuitive as EMG [5], [16], EIT [15], force-grip [6] or push-button [8] based interfaces, it gives to the operator the vital ability to independently command all aspects of the stiffness ellipsoid, which is a missing conceptual aspect of the state of the art interfaces.

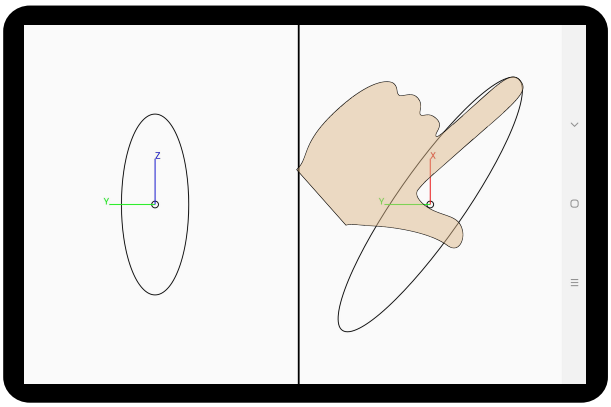

Fig. 2: The virtual ellipsoid interface for commanding robot endpoint stiffness realised using a touchscreen tablet device. The ellipsoid is shaped by a combination of index finger and thumb movements. The left-side section of the screen controls the ellipsoid in y-z plane of the world frame, while the right-side section controls the x-y plane. We aligned the world frame with the remote robot's base frame.

The scope of this paper is to introduce the novel method and present a proof-of-concept validation. We perform experiments on a Kuka LBR iiwa robotic arm (slave device) and a Force Dimension Sigma7 haptic device (master device). The experimental tasks involve two scenarios, in which impedance adjustments of the remote robot are required: counteracting unpredictable perturbations from the environment and establishing physical contact with unknown objects. Lastly, we assess the performance, usefulness and perceived workload of the designed impedance-command interface in a human subject experiment.

II. Method

An overview of the proposed method is illustrated in Fig. 1. The human operator holds the haptic device in one hand and controls the endpoint position and orientation of the remote robot by the movements of his/her arm. This paper's main contribution is a novel tele-impedance control interface that allows the human operator to independently and simultaneously change a virtual stiffness ellipsoid's size, shape and orientation in real-time with the other (free) hand (i.e., the hand that is not used for controlling the haptic device). The virtual ellipsoid is mapped in real-time to the Cartesian stiffness ellipsoid of the remote robot. The operator can then adapt the stiffness strategy based on his/her experience, cognitive capabilities, using the visual feedback of task environment or (if available) force-feedback [8]. The measured force at the remote robot can be used as a force-feedback to be reproduced at the human operator's arm by the haptic device to improve the intuitiveness [6], [8]–[10]; the methods in [10], [24] can be used to ensure stability and transparency. We performed the proof-of-concept experiments without force-feedback. This increased the task difficulty due to lack of tactile information, though these tests showed that tele-impedance can be successful even without force-feedback [5], [7].

A. Virtual Stiffness Ellipsoid Command Interface

The developed stiffness-command interface uses the proposed virtual ellipsoid method. The virtual ellipsoid was created and controlled through a touchscreen device as shown in Fig. 2. For this purpose, we used an off-the-shelf tablet. The screen of the tablet was split into two sections; each section showed a different point of view of the virtual ellipsoid in the world frame. The left section showed the view in the y-z plane (i.e., frontal plane from the human body perspective), while the right section showed the view in the x-y plane (i.e., horizontal plane from the human body perspective). Optionally, the current remote robot configuration can be additionally displayed on the tablet to give a better feeling about how the ellipsoid is oriented with respect to the endpoint, however, this was not done in the experiments to assume worst case scenario. Note that the proposed virtual ellipsoid method can be potentially implemented also on other (emerging) technologies, such as hologram, etc.

The human operator controls the size, shape and orientation of the virtual stiffness ellipsoid with the index and thumb fingers of the hand that is not used to control the haptic device. The principal vectors of the ellipsoid are calculated between the center point of the ellipse and each finger position at the point of contact with the screen. When the hand is in the left-side section (y-z plane), the index finger controls the new z-axis vector and the thumb controls the new y-axis of the ellipsoid. When the hand is in the right-side section (x-y plane), the index finger controls the new x-axis vector and the thumb controls the new y-axis of ellipsoid.

The principal axes of the virtual ellipsoid, as controlled by the human operator, are used to form a matrix

$$\boldsymbol{E} = \begin{bmatrix} e_x^x & e_y^x & e_x^x \\ e_x^y & e_y^y & e_z^y \\ e_x^z & e_y^z & e_z^z \end{bmatrix}, \tag{1}$$

where $\boldsymbol{E} \in \mathbb{R}^{3\times3}$ is the virtual ellipsoid matrix and e are elements of the principle axis vectors. The subscripts denote the principal axes of the desired ellipsoid and superscripts denote components of the vector with respect to the world frame. For example, e_x^y represents the y-axis component in the world frame of an ellipsoid's x principal axis in a rotated frame. As we measured the principal axes on a touchscreen, we expressed the principal axes $\boldsymbol{e}$ in pixels.

The virtual ellipsoid is then used to alter the remote robot's endpoint stiffness matrix according to

$$\boldsymbol{K}_T^{new} = \boldsymbol{V}\boldsymbol{\Sigma}\boldsymbol{K}_e\boldsymbol{V}^T, \tag{2}$$

where $\boldsymbol{K}_T^{new} \in \mathbb{R}^{3\times3}$ is the new translation part of stiffness matrix $\boldsymbol{K} \in \mathbb{R}^{6\times6}$, and where $\boldsymbol{\Sigma} \in \mathbb{R}^{3\times3}$ and $\boldsymbol{V} \in \mathbb{R}^{3\times3}$ are eigenvalues and eigenvectors of the virtual ellipsoid matrix obtained by eigen decomposition

$$\boldsymbol{E} = \boldsymbol{V}\boldsymbol{\Sigma}\boldsymbol{V}^T. \tag{3}$$

The eigenvectors are used to rotate the robot stiffness matrix in the world frame (aligned with the robot base frame) to match the virtual stiffness ellipsoid. The eigenvalues are used to control the stiffness values in different axes of the rotated frame. Diagonal factor matrix $\boldsymbol{K}_e \in \mathbb{R}^{3\times3}$ is used to convert geometrical units of the virtual ellipsoid vectors (e.g., pixels on a touch screen) into robot stiffness units. In our case, the units of $\boldsymbol{K}_e$ are N/(m · px).

The developed virtual ellipsoid interface has no means to control the magnitude of the robot's rotational stiffness yet. These values have to be preset. Nevertheless, the rotation of the robot stiffness ellipsoid in (2) has to be accounted for so that the orientation of the rotational axes matches the orientation of the new commanded translational axes. This is done through

$$\boldsymbol{K}_R^{new} = \boldsymbol{V}\boldsymbol{K}_R\boldsymbol{V}^T, \tag{4}$$

where $\boldsymbol{K}_R^{new} \in \mathbb{R}^{3\times3}$ is the new rotational part of the robot stiffness matrix $\boldsymbol{K} \in \mathbb{R}^{6\times6}$ and $\boldsymbol{K}_R \in \mathbb{R}^{3\times3}$ is a diagonal matrix, which elements preset the desired rotational stiffness in the world frame (aligned with the robot base frame). Both (2) and (4) must ensure that the resulting stiffness matrices are symmetric positive definite [4].

The full robot stiffness matrix is then obtained through

$$\boldsymbol{K} = \begin{bmatrix} \boldsymbol{K}_T^{new} & 0 \\ 0 & \boldsymbol{K}_R^{new} \end{bmatrix}. \tag{5}$$

B. Robot Controller for Physical Interaction

The remote robot's physically interactive behaviour was governed by a Cartesian impedance controller defined as

$$\boldsymbol{f} = \boldsymbol{K}\big(\boldsymbol{x}_r - \boldsymbol{x}_a\big) + \boldsymbol{D}\big(\dot{\boldsymbol{x}}_r - \dot{\boldsymbol{x}}_a\big), \tag{6}$$

where $\boldsymbol{f} \in \mathbb{R}^6$ is the endpoint force/torque acting from the robot on the environment, $\boldsymbol{x}_r \in \mathbb{R}^6$ and $\boldsymbol{x}_a \in \mathbb{R}^6$ are the reference and actual endpoint pose, respectively, $\boldsymbol{K} \in \mathbb{R}^{6\times6}$ is the Cartesian stiffness matrix and $\boldsymbol{D}_r \in \mathbb{R}^{6\times6}$ is the Cartesian damping matrix. Stiffness matrix $\boldsymbol{K}$ was continuously obtained from (5), while a *double diagonalisation design* [25] was used to form the damping matrix based on the current stiffness matrix as

$$\boldsymbol{D} = 2\boldsymbol{Q}\boldsymbol{D}_\xi\sqrt{\boldsymbol{K}_0}\boldsymbol{Q}^T, \tag{7}$$

where the $\boldsymbol{Q} \in \mathbb{R}^{6\times6}$ and $\boldsymbol{K}_0 \in \mathbb{R}^{6\times6}$ are eigenvectors and eigenvalues of the eigen decomposition of stiffness matrix $\boldsymbol{K} = \boldsymbol{Q}\boldsymbol{K}_0\boldsymbol{Q}^T$. The diagonal matrix $\boldsymbol{D}_\xi \in \mathbb{R}^{6\times6}$ contains damping ratios, which we set to 0.7.

The interaction force applied between the robot and the environment $\boldsymbol{f}$ from (6) was included into the robot torque control scheme by

$$\boldsymbol{\tau} = \boldsymbol{M}(\boldsymbol{q})\ddot{\boldsymbol{q}} + \boldsymbol{C}(\boldsymbol{q},\dot{\boldsymbol{q}})\dot{\boldsymbol{q}} + \boldsymbol{g}(\boldsymbol{q}) + \boldsymbol{J}^T(\boldsymbol{q})\boldsymbol{f}, \tag{8}$$

where $\boldsymbol{\tau} \in \mathbb{R}^6$ is a vector of robot joint torques, $\boldsymbol{q} \in \mathbb{R}^7$ is a vector of robot joint angles, $\boldsymbol{J} \in \mathbb{R}^{6x7}$ is the robot arm Jacobian matrix, $\boldsymbol{M} \in \mathbb{R}^{6\times6}$ is the robot mass matrix, $\boldsymbol{C} \in \mathbb{R}^{6\times6}$ is the Coriolis and centrifugal matrix and $\boldsymbol{g} \in \mathbb{R}^6$ is the gravity vector. The robot was torque-controlled and $\boldsymbol{\tau}$ was used as an input.

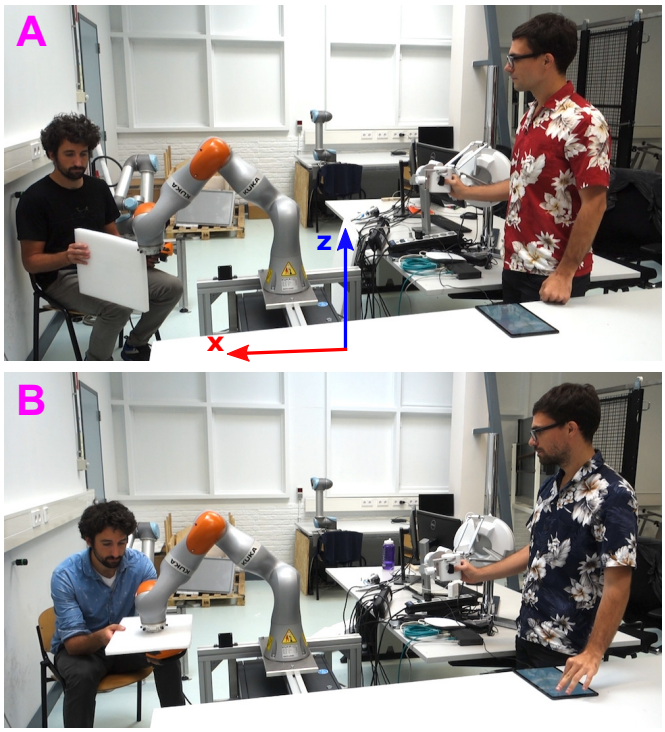

Fig. 3: Illustration of the concept demonstration experiments. The human operator controls the robotic arm through the haptic device and the virtual stiffness ellipsoid. The top photo (A) shows the external perturbation experiment. We introduced physical perturbations on the robot endpoint, simulating external perturbations of the environment. The bottom photo (B) shows the establishing contact experiment. We held an object on which contact had to be established. The world frame orientation is illustrated by the red arrow for the x-axis and blue arrow for the z-axis, while the y-axis follows the right-handed coordinate system. The robot base frame was aligned with the world frame.

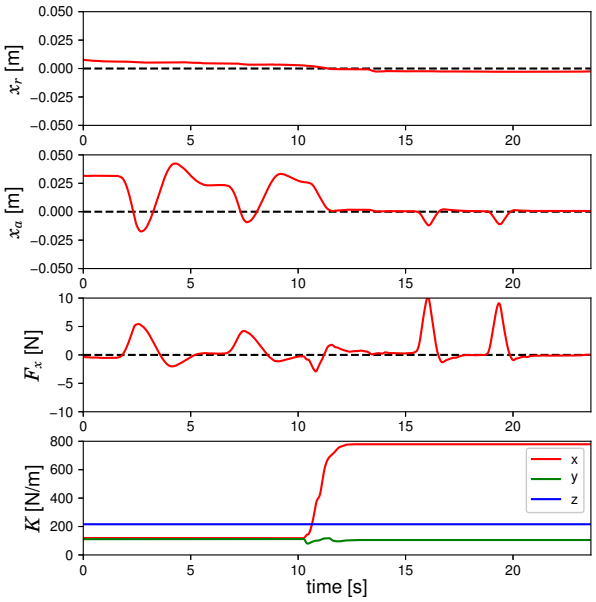

Fig. 4: Results of the perturbation experiment. The top graph shows the reference position in the direction of perturbation (robot base frame x-axis). The second graph shows the actual position. The third graph shows the force that the robot exerted in the direction of external disturbance. The third graph shows the force that the robot exerted. The last graph shows the principal components of robot stiffness in its base frame.

III. Concept Demonstration Experiments

To validate the proposed stiffness-command interface for tele-impedance, we performed a series of experiments on a setup that included a Kuka LBR iiwa robotic arm (7 DoF), a Force Dimension Sigma7 haptic device (7 DoF) and the novel virtual ellipsoid interface generated on a Samsung Galaxy Tab with a 10.5-inch touchscreen. The proposed virtual ellipsoid method, described in Section II-A, was implemented through a custom-written Android application. The robotic arm was controlled by the impedance controller as described in Section II-B. The stiffness-command interface, haptic interface and the robotic arm communicated through a UDP protocol. The experiments involved two common types of tasks, in which changing the stiffness of the robot is crucial for safe and successful task execution. To define and adjust the commanded stiffness strategy, the operator primarily relied on experience, cognitive capabilities and visual feedback.

The goal of the first task was controlling the robot position while at the same time counteracting unpredictable external perturbations (see Fig. 3A). Ideally, the robot should be compliant in order to operate safely in the vicinity of a human or in an unstructured environment. However, when the robot is exposed to external perturbations, it cannot remain complaint in the direction of perturbations, if we wish the robot to track the commanded reference position in a satisfactory manner. In such a case, the robot needs to stiffen up in the direction of the perturbations to improve the position tracking.

The goal of the second task was to approach and establish a physical contact with an object (see Fig. 3B). If the properties of the object (e.g., stiffness) or its exact position are unknown a-priori – either through a lack of models of the environment, unpredictable factors like a collaborating human or a lack of reliable sensory information – approaching the object with high endpoint stiffness is unsafe and the robot might damage the object, harm the collaborating human or itself due to excessive interaction forces. In such a case, the robot should ideally decrease the stiffness in the direction of the approach and contact in order to maximise safety. Even if the reference position goes beyond the object due to poor estimation of its position by the human operator, the difference between the reference and the actual position of the robot (actual position remains on the object surface) is only multiplied by a small gain (i.e., a small stiffness value) and, therefore, resulting in a relatively small interaction force (according to the impedance control law (6)).

The available touchscreen area on either left-side or right-side section was 800 pixels. Factor matrix $\boldsymbol{K}_e$ was set 1.0 N/(m$\cdot$px), enabling the human operator to control maximum translational stiffness of the remote robot to 800 N/m in each direction of Cartesian space. Rotational stiffness matrix $\boldsymbol{K}_R$ was preset to 50 Nm/rad around all three axes in the Cartesian space. Note that rotation of the virtual ellipsoid changes the rotational matrix according to (2).

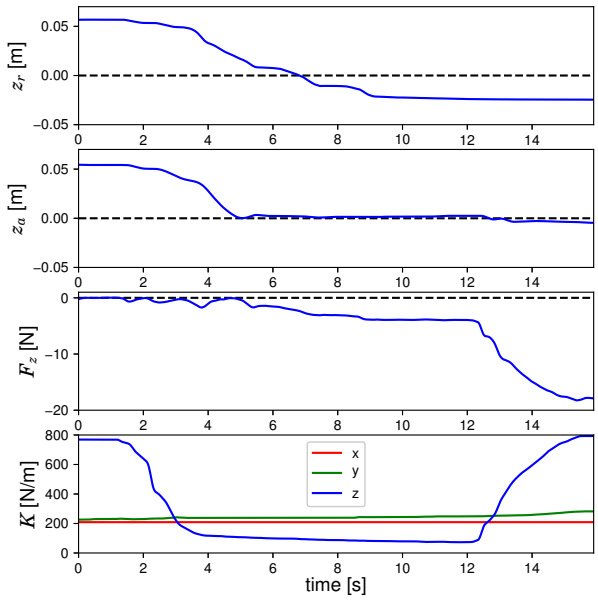

Fig. 5: Results of the contact establishing experiment. The top graph shows the reference position in the z-axis of the robot base frame. The second graph shows the actual position. The third graph shows the force that the robot exerted on the object. The last graph shows the principal components of robot stiffness in its base frame.

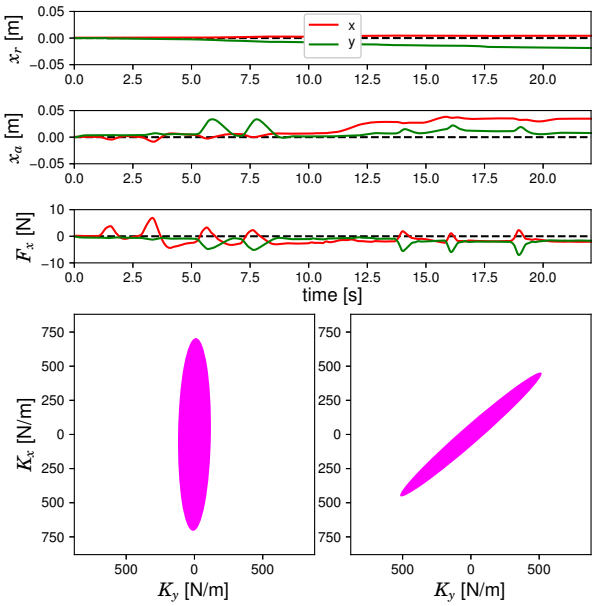

Fig. 6: Results of the ellipsoid orientation adjustment experiment. The top graph shows the reference position in x-axis and y-axis of the robot base frame. The perturbation was not aligned with any of the axes and was coming at 45° angle with respect to x-y plane. The second graph shows the actual position. The third graph shows the interaction force. The last graph shows the robot stiffness ellipsoids in the first and the second phase of the experiment.

A. *Task 1: External Perturbation*

The results of the experiment are shown in Fig. 4. The human operator commanded a reference position of the remote robotic arm (see the top graph). Initially, the stiffness was set to a low value in all three axes of the robot base frame (see the last graph) to maximise safety. In this experiment, the stiffness ellipsoid was not rotated with respect to the robot base frame, so $\boldsymbol{K}$ was diagonal and the graph shows the stiffness components in the principal directions of the robot base frame. Note how the position tracking was less precise when the stiffness was low due to imperfections in the robot's forward dynamics model.

A human assistant was near the remote robot and introduced perturbations at its endpoint in the x-axis of the robot base frame. The force of perturbation is visible in the third graph, while the corresponding displacement of actual robot position is visible in the second graph. When the human operator noticed the perturbations that were disturbing the position tracking task in x-axis, he used the proposed virtual ellipsoid interface to reshape the robot stiffness ellipsoid online in a way that it became stiffer in the direction of the perturbation. This happened at 10 seconds in the experiment (see the last graph).

After increasing the stiffness, tracking of the commanded reference position became much stricter, as it can be observed in the second graph after the 10th second of the experiment. The human assistant continued with the perturbations. However, now the displacement in the actual position were now much smaller, even though he increased the perturbation force. This is clearly visible when comparing the first half of experiment with the second half of experiment (second and third graphs).

B. *Task 2: Establishing Contact*

The results of the experiment are shown in Fig. 5. The human operator commanded a reference position of the remote robotic arm (see the top graph). Initially, the stiffness was set to a high value in z-axis of the robot base frame (see the last graph). Like before, in this experiment, the stiffness ellipsoid was not rotated with respect to the robot base frame, therefore $\boldsymbol{K}$ was diagonal and the graph shows the stiffness components in the principal directions of the robot base frame.

The human assistant was again near the remote robot and held a fragile but quite stiff object. The task of the human operator was to establish a contact between the robot endpoint and the object (this generic example can relate to many common human-robot collaboration tasks). The human operator used his cognitive ability and experience, which dictated that approaching unknown fragile objects or human with high stiffness may be dangerous and he therefore reduced the robot stiffness along the approach axis to a very low value (see the last graph). Because the interface worked in real-time, this could be done simultaneously with movement of the robot (see first and second graphs).

The moment the contact with the object was established, the initial impact force was very low (see the third graph). When contact was established safely, the human operator could then increase the commanded reference position inside the object in order to produce the desired interaction force (between 9 and 12 seconds in the experiment). Note that actual position did not move with the commanded reference position because the object blocked it.

Finally, to demonstrate that the interaction force can

Fig. 7: The push-button interface used to command robot endpoint stiffness from [8], [26]. Because the original interface could only scale the size of the stiffness ellipsoid in all directions simultaneously, we upgraded it with a multi-modal system, where the user can switch the modes for scaling orientation and major and minor axes. The upgraded push-button interface is comparable in price and applicability to the novel tablet interface and is therefore used a benchmark in the multi-subject analysis.

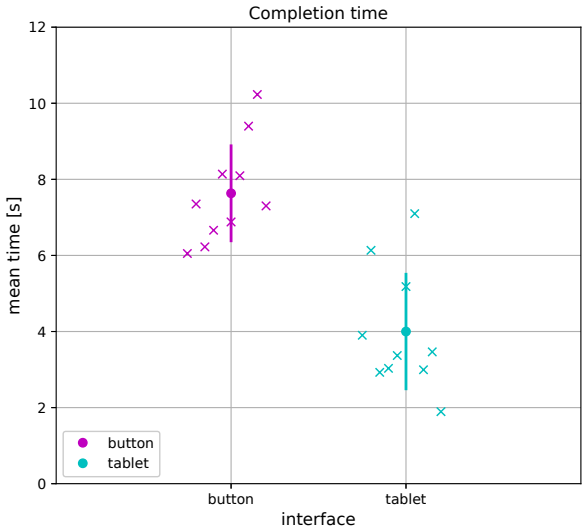

Fig. 8: Task completion time results of the human subject experiment. The purple symbols are associated with the push-button interface, while the cyan symbols are associated with the tablet interface. The dot represents the mean completion time, while the vertical line represents the standard deviation. The individual subject means are marked by crosses.

be controlled by a combination of reference position and stiffness according to (6), the human operator used the virtual ellipsoid interface to increase stiffness while maintaining the previous reference position. Note how the interaction force increased in magnitude after around 12 seconds, indicating the moment of contact with the object.

C. Task 3: Ellipsoid Orientation Adjustment

The results of the experiment are shown in Fig. 6. All variables are in the robot base frame. The scenario was similar to the perturbation experiment described above. However, here we wanted to demonstrate the ability of human operator to change the rotation of robot stiffness ellipsoid in real-time manner by using the virtual stiffness ellipsoid interface. The human assistant perturbed the robot in a direction that was not aligned with any of the axes of the robot base frame. The perturbation force can be observed in the third graph. Note how the direction of the perturbation can be derived from a combination of force in x-axis and y-axis of the robot base frame. Since it is roughly equal in both axes, the perturbation was coming at about 45° angle with respect to the robot base frame.

When the human operator noticed this perturbation, he changed the orientation of robot stiffness ellipsoid so that its major axis was aligned with the direction of the disturbance. The stiffness ellipsoid before the change is shown at the bottom left graph, while the stiffness ellipsoid after the change is shown at the bottom right graph. As a result, the actual position displacement became much lower, compared to the case before the orientation adjustment.

IV. Assessment of Interface Performance, Usability and Workload

A. Experiment methods

We performed a human subject experiment to analyse the performance, usability and experienced workload of the proposed method in comparison with another state-of-the-art method. We considered two other methods for controlling the remote robot's endpoint impedance: through an EMG-based interface, a grip-force interface or a push-button interface. As described in Section I, it is not possible to control all aspects of the remote robot's endpoint independently through EMG-based and grip-force interfaces, due to the human arm configuration dependency and neuro-mechanical properties. Furthermore, EMG has a limited applicability in real-world scenarios due to expensive hardware, reliance on wearable devices, and complicated and time-consuming calibration process. Therefore, we decided to use the push-button interface as a comparison to our proposed touchscreen interface, since it is comparable in terms of applicability and cost.

Nevertheless, one DoF push-button interface can only control either the size, shape or orientation at a time. We, therefore, modified the push-button interface [8], [26] (see Fig. 7) by adding a mode switching system, in which the subjects selected whether they wanted to control size, shape or orientation of the stiffness ellipsoid. The modes could be switched by a keyboard or verbal command, for simplicity we used three buttons on a keyboard to switch modes. Once a mode was selected, for example to change the size of the stiffness ellipsoid, the push button was used to change the associated parameter.

Ten subjects participated in the experiments with average age 27.0 ± 3.16. Prior to their participation the participants were familiarised with the study and experiment setup and signed an informed consent. The study was approved by the Human Research Ethics Committee of Delft University of Technology.

The subjects were instructed to match several reference stiffness ellipsoids displayed on a computer screen using both interfaces. There were five reference ellipsoids with different sizes, shapes and orientations. Each reference ellipsoid appeared three times during the main trial (15 in total) in a

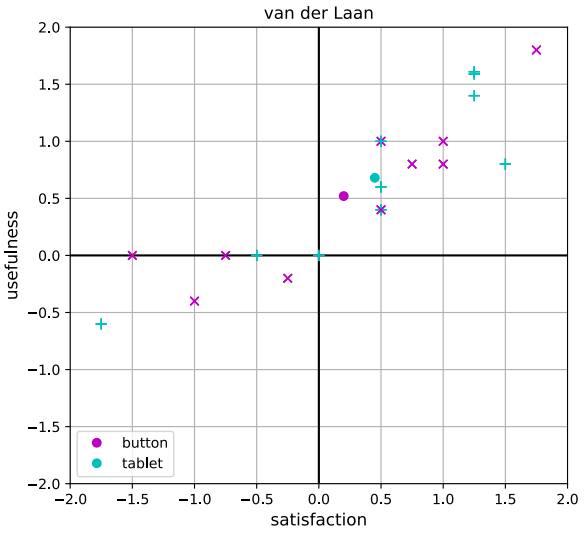

Fig. 9: Perceived usefulness versus satisfaction for both interface types, obtained using the van der Laan questionnaire. The purple colour is associated with the push-button interface, while the cyan colour is associated with the tablet interface. The dot represents the mean score on a satisfaction-usefulness plane. The individual subject data points are marked by crosses.

random order. The actual commanded ellipsoid was rendered in real-time on the same screen and were controlled by using the push-button interface or the tablet interface. Each interface represented one of the two experiment conditions, which were performed in two separate main trials. The order in which the two condition were performed was counterbalanced across subjects. Prior to each main trial, the subjects received instructions and performed a training trial in order to familiarise themselves with each input device. Only the main trials were used in the data analysis.

To assess matching performance, we measured the completion time that took the subjects to match each reference ellipsoid within a 5% error for three parameters that define the reference ellipsoids in a plane: orientation angle, minor axis length and major axis length. We calculated each subject's mean completion time, which were compared across the two interface types using dependent-samples t-tests ($\alpha = 0.05$). In addition, we used the *van der Laan* questionnaire [27] to assess interface usefulness and satisfaction and the *NASA-TLX* [28] questionnaire to assess workload (mental demand, physical demand, temporal demand, effort and frustration).

B. Results

On average, the subject swere much faster in forming the reference stiffness ellipsoids with the tablet interface compared to the push-button interface (see Fig. 8). The difference was statistically significant ($p < 0.001$).

Fig. 9 shows that the subjects perceived both interfaces to be somewhat satisfying and useful. The tablet interface scores slightly better on both scales; however, the difference was not statistically significant for either satisfaction ($p = 0.654$) or usefulness ($p = 0.631$).

The results of the NASA-TLX questionnaire are shown in Fig. 10. In general, the subjects perceived a good performance for both interfaces. All scores showed a considerable

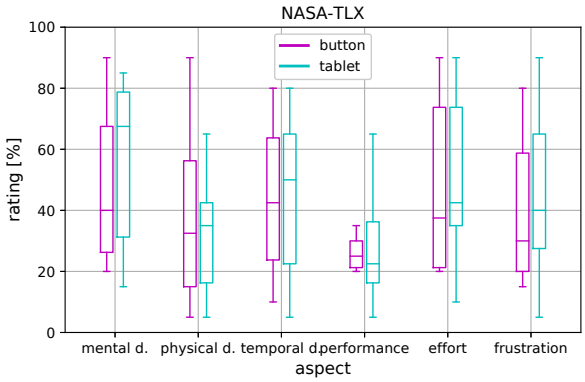

Fig. 10: Perceived workload results using NASA-TLX questionnaire for both input interfaces. The purple colour is associated with the push-button interface, while the cyan colour is associated with the tablet interface. The box-whisker plots depict median (horizontal line inside the box), interquartile range (box) and extreme values (whisker) for a given variable. Note that a lower value indicates a better condition for all aspects (e.g., lower mental demand, etc.), including for the perceived performance.

variation in for all aspects. No aspect yielded a significant difference between the push-button interface and the tablet interface.

V. Discussion

The result of the experiments demonstrated that the proposed stiffness-command interface can be a viable alternative to the existing state-of-the-art interfaces. The main advantage of the proposed method is that facilitate the control of all aspects of the stiffness ellipsoid independently, while state-of-the-art interfaces [5], [8], [11], [16] lack this conceptual feature. The developed interface can be implemented on any type of touchscreen device (even low-cost smartphones), which could significantly increase the application potential and accessibility to various users. Furthermore, the proposed virtual ellipsoid concept can be extended to other (emerging) technologies, such as hologram, etc.

The results of the human subject experiment show that the subjects were significantly faster in shaping the stiffness ellipsoid to a desired shape, size and orientation using the touchscreen interface compared to a push-button interface. On average, the subjects judged the proposed interface relatively satisfactory and useful. A few subjects indicated that coordinating the fingers with respect to the touchscreen was challenging, however, most of them were able to do it sufficiently well with practice. One subject commented that he was not familiar with tablet devices and would have preferred more training. Based on this, we suspect that some of the frustration came from too little training, therefore, we recommend that operators are sufficiently trained prior to using the interface. The perceived workload showed a considerable variability, which should be further investigated in future work.

A potential disadvantage of the proposed interface is that it could require more attention from the human operator and might therefore be less intuitive compared to some of the existing interfaces. Using EMG [5], [9], EIT [15] or grip-force [11] based interfaces, the human might naturally

contract its muscles based on the situation in the remote environment, which in turn would change the remote robot's endpoint stiffness, as shown in [21]. Therefore, the proposed method might be more suitable for application in space or industrial robotics, where changes tend to be slower, while the above-mentioned methods might be more suitable for application in robotic surgery, where quick stiffness changes are crucial. However, a sufficient training might improve the use of proposed virtual stiffness ellipsoid method. Another limitation becomes evident when a dual-arm teleoperation is required, where both hands required to control the motion of two remote robotic arms.

The scope of this paper was to introduce the novel method and perform proof-of-concept validation experiments. In the future, we will focus on going beyond the proof-of-concept validation, improve the interface considering usability and workload and perform various supplementary experiments, such as experimental comparison between other existing methods. One potentially interesting direction would be to explore the human attention required for using different interfaces.

The interface introduced in this paper focused on applicability by stressing on low-cost and high amount of controllability, at some expense of intuitiveness. In future we will explore other derivations of the proposed concept. For example, we could develop a 3 DoF representation of the stiffness ellipse instead of the segmented 2 DoF visual representation we proposed here. In addition, we will develop a more complex haptic version of the same concept in which the human operator can actually feel the shape of the ellipsoid.

ACKNOWLEDGMENTS

The authors would like to thank Yu-Chih Huang for her help with programming the touchscreen tablet application.

REFERENCES

[1] N. Hogan, "Adaptive control of mechanical impedance by coactivation of antagonist muscles," *Automatic Control, IEEE Transactions on*, vol. 29, no. 8, pp. 681–690, Aug 1984.

[2] E. Burdet, R. Osu, D. W. Franklin, T. E. Milner, and M. Kawato, "The central nervous system stabilizes unstable dynamics by learning optimal impedance," *Nature*, vol. 414, no. 6862, pp. 446–449, Nov. 2001.

[3] T. Tsumugiwa, R. Yokogawa, and K. Hara, "Variable impedance control with virtual stiffness for human-robot cooperative peg-in-hole task," in *2002 IEEE/RSJ International Conference on Intelligent Robots and Systems (IROS)*, vol. 2, 2002, pp. 1075–1081.

[4] L. Peternel, N. Tsagarakis, and A. Ajoudani, "A human-robot co-manipulation approach based on human sensorimotor information," *IEEE Transactions on Neural Systems and Rehabilitation Engineering*, vol. 25, no. 7, pp. 811–822, July 2017.

[5] A. Ajoudani, N. G. Tsagarakis, and A. Bicchi, "Tele-impedance: Teleoperation with impedance regulation using a body-machine interface," *The International Journal of Robotics Research*, vol. 31, no. 13, pp. 1642–1656, 2012.

[6] D. S. Walker, "Design of versatile telerobotic systems using variable impedance actuation and control," Ph.D. dissertation, Stanford University, 2013.

[7] L. Peternel, T. Petrič, E. Oztop, and J. Babič, "Teaching robots to cooperate with humans in dynamic manipulation tasks based on multi-modal human-in-the-loop approach," *Autonomous robots*, vol. 36, no. 1-2, pp. 123–136, Jan 2014.

[8] L. Peternel, T. Petrič, and J. Babič, "Robotic assembly solution by human-in-the-loop teaching method based on real-time stiffness modulation," *Autonomous Robots*, vol. 42, no. 1, pp. 1–17, Jan 2018.

[9] C. Yang, C. Zeng, P. Liang, Z. Li, R. Li, and C. Su, "Interface design of a physical humanrobot interaction system for human impedance adaptive skill transfer," *IEEE Transactions on Automation Science and Engineering*, vol. 15, no. 1, pp. 329–340, Jan 2018.

[10] M. Laghi, A. Ajoudani, M. G. Catalano, and A. Bicchi, "Unifying bilateral teleoperation and tele-impedance for enhanced user experience," *The International Journal of Robotics Research*, vol. 39, no. 4, pp. 514–539, 2020.

[11] D. Walker, J. Salisbury, and G. Niemeyer, "Demonstrating the benefits of variable impedance to telerobotic task execution," in *2011 IEEE International Conference on Robotics and Automation (ICRA)*, May 2011, pp. 1348–1353.

[12] C. Yang, G. Ganesh, S. Haddadin, S. Parusel, A. Albu-Schäffer, and E. Burdet, "Human-like adaptation of force and impedance in stable and unstable interactions," *Robotics, IEEE Transactions on*, vol. 27, no. 5, pp. 918–930, Oct 2011.

[13] J. Buchli, F. Stulp, E. Theodorou, and S. Schaal, "Learning variable impedance control," *Int. J. Rob. Res.*, vol. 30, no. 7, pp. 820–833, Jun 2011.

[14] F. J. Abu-Dakka, L. Rozo, and D. G. Caldwell, "Force-based variable impedance learning for robotic manipulation," *Robotics and Autonomous Systems*, vol. 109, pp. 156–167, 2018.

[15] E. Zheng, Y. Li, Z. Zhao, Q. Wang, and H. Qiao, "An electrical-impedance-tomography-based interface for human-robot collaboration," *IEEE/ASME Transactions on Mechatronics*, 2020.

[16] A. Ajoudani, C. Fang, N. Tsagarakis, and A. Bicchi, "Reduced-complexity representation of the human arm active endpoint stiffness for supervisory control of remote manipulation," *The International Journal of Robotics Research*, vol. 37, no. 1, pp. 155–167, 2018.

[17] A. Ajoudani, N. G. Tsagarakis, and A. Bicchi, "Choosing poses for force and stiffness control," *IEEE Transactions on Robotics*, vol. 33, no. 6, pp. 1483–1490, Dec 2017.

[18] G. Torres-Oviedo and L. H. Ting, "Muscle synergies characterizing human postural responses," *Journal of neurophysiology*, vol. 98, no. 4, pp. 2144–2156, 2007.

[19] M. T. Turvey, "Action and perception at the level of synergies," *Human movement science*, vol. 26, no. 4, pp. 657–697, 2007.

[20] M. Ison and P. Artemiadis, "The role of muscle synergies in myoelectric control: trends and challenges for simultaneous multifunction control," *Journal of neural engineering*, vol. 11, no. 5, p. 051001, 2014.

[21] L. M. Doornebosch, D. A. Abbink, and L. Peternel, "Analysis of coupling effect in human-commanded stiffness during bilateral tele-impedance," *IEEE Transactions on Robotics*, vol. 37, no. 4, pp. 1282–1297, 2021.

[22] Y. Gao, H. Li, and Y. Luo, "An empirical study of wearable technology acceptance in healthcare," *Industrial Management & Data Systems*, 2015.

[23] J. V. Jacobs, L. J. Hettinger, Y.-H. Huang, S. Jeffries, M. F. Lesch, L. A. Simmons, S. K. Verma, and J. L. Willetts, "Employee acceptance of wearable technology in the workplace," *Applied ergonomics*, vol. 78, pp. 148–156, 2019.

[24] D. A. Lawrence, "Stability and transparency in bilateral teleoperation," *IEEE Transactions on Robotics and Automation*, vol. 9, no. 5, pp. 624–637, Oct 1993.

[25] A. Albu-Schäffer, C. Ott, U. Frese, and G. Hirzinger, "Cartesian impedance control of redundant robots: recent results with the DLR-light-weight-arms," in *2003 IEEE International Conference on Robotics and Automation (ICRA)*, Sept 2003, pp. 3704–3709.

[26] L. Peternel, T. Petrič, and J. Babič, "Human-in-the-loop approach for teaching robot assembly tasks using impedance control interface," in *2015 IEEE International Conference on Robotics and Automation (ICRA)*, May 2015, pp. 1497–1502.

[27] J. D. Van Der Laan, A. Heino, and D. De Waard, "A simple procedure for the assessment of acceptance of advanced transport telematics," *Transportation Research Part C: Emerging Technologies*, vol. 5, no. 1, pp. 1–10, 1997.

[28] S. G. Hart and L. E. Staveland, "Development of nasa-tlx (task load index): Results of empirical and theoretical research," in *Advances in psychology*. Elsevier, 1988, vol. 52, pp. 139–183.